

Strong spin-orbit fields and Dyakonov-Perel spin dephasing in supported metallic films

Nguyen H. Long,* Phivos Mavropoulos,† David S. G. Bauer, Bernd Zimmermann, Yuriy Mokrousov, and Stefan Blügel

*Peter Grünberg Institut and Institute for Advanced Simulation,
Forschungszentrum Jülich and JARA, D-52425 Jülich, Germany*

(Dated: August 29, 2018)

Spin dephasing by the Dyakonov-Perel mechanism in metallic films deposited on insulating substrates is revealed, and quantitatively examined by means of density functional calculations combined with a kinetic equation. The surface-to-substrate asymmetry, probed by the metal wave functions in thin films, is found to produce strong spin-orbit fields and a fast Larmor precession, giving a dominant contribution to spin decay over the Elliott-Yafet spin relaxation up to a thickness of 70 nm. The spin dephasing is oscillatory in time with a rapid (sub-picosecond) initial decay. However, parts of the Fermi surface act as spin traps, causing a persistent tail signal lasting 1000 times longer than the initial decay time. It is also found that the decay depends on the direction of the initial spin polarization, resulting in a spin-dephasing anisotropy of 200% in the examined cases.

PACS numbers: 72.25.Rb, 73.50.Bk, 72.25.Ba, 85.75.-d

In spintronics experiments, spins are often excited in, or transported through, non-magnetic metallic thin film media [1]. Typical examples are Cu, Au or Pt, used in spin-current creation or detection via the spin Hall effect [2–5] or spin Nernst effect [6, 7]. Paramount for the spin-transport properties of a medium is the characteristic time T after which the out-of-equilibrium spin population that was created in the medium is lost by relaxation or dephasing [8, 9]. The microscopic mechanisms leading to spin reduction depend on the material properties, and it is commonly accepted that the Elliott-Yafet (EY) mechanism [10, 11] is dominant in metals [12–15], since they show space-inversion symmetry [16]. However, any substrate on which the film is deposited breaks the inversion symmetry; if the film is thin enough (thinner than the electron phase relaxation length), the resulting asymmetry is felt by the metallic states extending over the film thickness, even though the substrate and surface potential are screened in the film interior. In this case, as we argue in this Letter, the band structure changes throughout the film and the Dyakonov-Perel (DP) mechanism [17] for spin dephasing is activated and becomes the dominant cause of spin reduction. The DP mechanism (that we briefly describe below) is known to be important in III-V or II-VI semiconductors or semiconductor heterostructures due to their inversion asymmetry [18, 19], but, to our knowledge, it has been completely overlooked so far in the important case of metallic films.

Characteristic of systems with spin-orbit coupling and time reversal symmetry but broken inversion symmetry is the lifting of *conjugation* degeneracy [11] at each crystal momentum \mathbf{k} and energy $E_{\mathbf{k}}$ of the band structure. The resulting pair of states $\Psi_{\mathbf{k}}^{\pm}$ obtains energies $E_{\mathbf{k}}^{\pm}$ with the (usually small) splitting $\hbar|\Omega_{\mathbf{k}}| = E_{\mathbf{k}}^{+} - E_{\mathbf{k}}^{-}$ depending on the spin-orbit strength, the strength of the antisymmetric part of the potential V_A , and the overlap of the wavefunction $\Psi_{\mathbf{k}}$ with V_A . The situation is described by adding to the \mathbf{k} -dependent crystal Hamiltonian the term

$$\Delta H(\mathbf{k}) = \frac{\hbar}{2} \Omega_{\mathbf{k}} \cdot \boldsymbol{\sigma} \quad (1)$$

where $\boldsymbol{\sigma}$ is the vector of Pauli-matrices and the vector quantity

$\Omega_{\mathbf{k}}$ is called the *spin-orbit field* (SOF) [8, 20]. The direction of $\pm\Omega_{\mathbf{k}}$ is given by the direction of the spin expectation value of $\Psi_{\mathbf{k}}^{\pm}$.

From this well-known theory follows the Dyakonov-Perel mechanism of spin dephasing. In brief, one assumes that an electron wavepacket at wave vector \mathbf{k} with a given spin direction $\mathbf{s}_{\mathbf{k}}$ is composed of a superposition of $\Psi_{\mathbf{k}}^{\pm}$. Then, effectively, $\Omega_{\mathbf{k}}$ will act on the spin as a magnetic field due to Eq. (1) and $\mathbf{s}_{\mathbf{k}}$ will precess around $\Omega_{\mathbf{k}}$. After an average momentum lifetime T_p , the electron is scattered with a transition rate $P_{\mathbf{k}'\mathbf{k}}$ to \mathbf{k}' occupying a superposition of $\Psi_{\mathbf{k}'}^{\pm}$ (the scattering is assumed to be energy- and spin-conserving) and precesses around $\Omega_{\mathbf{k}'}$, etc. Since the scattering sequence is a stochastic process, the electron spin effectively precesses around a sequence of random axes and the information on the initial direction of $\mathbf{s}_{\mathbf{k}}$ is finally lost after a characteristic Dyakonov-Perel time of T_{DP} . The process is governed by a kinetic equation [20]:

$$\frac{\partial \mathbf{s}_{\mathbf{k}}}{\partial t} = \Omega_{\mathbf{k}} \times \mathbf{s}_{\mathbf{k}} - \sum_{\mathbf{k}'} P_{\mathbf{k}'\mathbf{k}} (\mathbf{s}_{\mathbf{k}} - \mathbf{s}_{\mathbf{k}'}). \quad (2)$$

The occupation of $\Psi_{\mathbf{k}}^{\pm}$ by a single wavepacket implies that the splitting $\hbar|\Omega_{\mathbf{k}}|$ is small: one can conceive a wavepacket of large energy spread, but it is unlikely that after several scattering events both $\Psi_{\mathbf{k}}^{\pm}$ will follow the same path in \mathbf{k} -space if their energy difference is large. In this sense, we expect that the Rashba surface states of metals, being in many cases characterized by a large $\hbar|\Omega_{\mathbf{k}}|$ [e.g. of the order of 100 meV at the Fermi level for Au(111) [21, 22]], will produce strong spin relaxation but not follow the DP mechanism.

In the present Letter we demonstrate the importance of the DP mechanism in metallic films deposited on insulating substrates. We use the density-functional-based Korringa-Kohn-Rostoker (KKR) Green function method for the calculation of the band structure and transition rates [23–25], and Eq. (2) for the time evolution of the spin expectation value. In our calculations we explicitly assume that all scattering is caused by self-atom impurities, that are always present on metal surfaces; the concept that we demonstrate, however, is valid

also in the presence of other scattering sources and can be easily quantified if the transition rate is known. As we find, the dephasing process is controlled by an interplay between film thickness, scattering strength, and penetration depth of the film wavefunctions into the insulating substrate and into the vacuum.

In the following, we give a short description of our method of calculation of spin-orbit fields, focussing on the basic principles and the approximations [26]. In a metallic film of thickness d deposited on an insulating substrate, the wavefunctions $\Psi_{\mathbf{k}}$ around the Fermi energy probe the surface and substrate potential, V_{surf} at $z > d/2$ and V_{sub} at $z < -d/2$, only by exponentially evanescent tails ($z = 0$ defines the film mid-plane). Since by assumption, the free-standing film shows inversion symmetry, the antisymmetric part of the potential is just $V_A(\mathbf{r}) = \frac{\text{sign}(z)}{2}[V_{\text{surf}}(\mathbf{r}) - V_{\text{sub}}(-\mathbf{r})]$. The smallness of the overlap ($\langle \Psi_{\mathbf{k}}, V_A \Psi_{\mathbf{k}} \rangle \propto 1/d$) allows us to calculate $\Omega_{\mathbf{k}}$ in linear response to V_A with the free-standing film as a reference (the linear approximation improving at larger thicknesses). In a second, simplifying step, the substrate is mimicked by a constant barrier V_0 added to the surface potential of the free-standing film at $z < -d/2$, yielding $V_A = -\frac{\text{sign}(z)}{2}V_0\theta(|z| - d/2)$. The conceptual advantage of this approximation is that one can define spin-orbit fields characteristic of the free-standing film, where the substrate enters only via a linear multiplicative factor V_0 . I.e., one obtains the linear relation

$$\Omega_{\mathbf{k}} = V_0 \omega_{\mathbf{k}}, \quad (3)$$

where the *spin-orbit field susceptibility* $\omega_{\mathbf{k}}$ was introduced. The value of $\omega_{\mathbf{k}}$ can be calculated in linear response theory on the basis of the free-standing film, while the parameter V_0 can be fitted at high symmetry points in the Brillouin zone for any given substrate with respect to an explicit calculation of the film on the substrate. We consider this second step well suited for a qualitative discussion, while the exact values of $\Omega_{\mathbf{k}}$ can deviate somewhat from this result. Quantitative improvements by taking the full substrate potential explicitly into account are possible but numerically expensive and are not necessary to unravel the general phenomenon which is the motivation here.

In solving Eq. (2) for the spin population $\mathbf{s}_{\mathbf{k}}(t)$, we assume that the excited electron concentration is small, so that the scattering is practically not affected by the final state occupation, and that the excited states are close to the Fermi level, confining in practice the \mathbf{k} values to the Fermi surface (FS). As an initial condition at $t = 0$, we choose that $\mathbf{s}_{\mathbf{k}}$ is along the positive z axis, i.e. normal to the film surface. Other choices of initial conditions, corresponding to different physical situations, are of course possible. A Fermi surface integration gives us the sought-for quantity $\langle s_z(t) \rangle = (1/n_F) \sum_{\mathbf{k}} (\mathbf{s}_{\mathbf{k}}(t))_z$, i.e., the magnetization along the initial axis z , normalized to the density of states n_F at the Fermi level. We assume that we are in the low concentration regime, i.e., $P_{\mathbf{k}\mathbf{k}'}$ scales linearly to the impurity concentration. Even under this assumption,

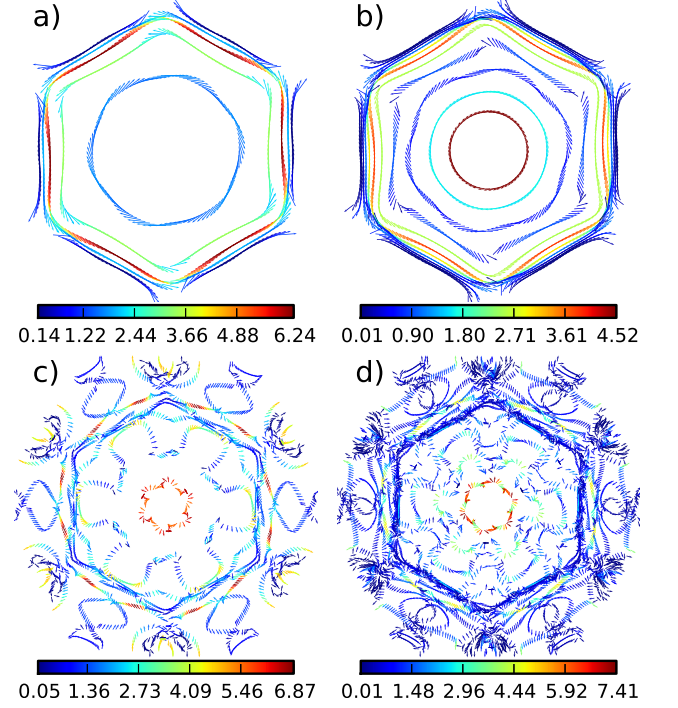


FIG. 1: (Color online) The distribution of the spin-orbit field susceptibility $\omega_{\mathbf{k}}$ on the Fermi surfaces of a) 6-layer Au(111), b) 12-layer Au(111), c) 6-layer Pt(111) and d) 12-layer Pt(111) films. The arrows denote the projection of the direction of the spin-orbit fields onto the surface plane. The color code denotes the absolute value of $\hbar|\omega_{\mathbf{k}}| \times 10^3$. The surface states are not shown. See the supplemental material for plots with improved resolution.

the solution of Eq. (2) has no simple scaling properties with respect to concentration or to V_0 . Eq. (2) has to be explicitly solved for each set of these parameters.

We also compare the DP with the EY mechanism that neglects precession but accounts for spin-flip scattering. We employ the master equation for the spin-dependent electron distribution function $n_{\mathbf{k}}^{\sigma}(t)$ involving spin-conserving and spin-flip transition rates $P_{\mathbf{k}\mathbf{k}'}^{\sigma\sigma'}$ [26],

$$\frac{dn_{\mathbf{k}}^{\sigma}}{dt} = \sum_{\mathbf{k}'} [P_{\mathbf{k}\mathbf{k}'}^{\sigma\sigma} n_{\mathbf{k}'}^{\sigma} + P_{\mathbf{k}\mathbf{k}'}^{\sigma\bar{\sigma}} n_{\mathbf{k}'}^{\bar{\sigma}} - P_{\mathbf{k}'\mathbf{k}}^{\sigma\sigma} n_{\mathbf{k}}^{\sigma} - P_{\mathbf{k}'\mathbf{k}}^{\bar{\sigma}\sigma} n_{\mathbf{k}}^{\sigma}], \quad (4)$$

where $\bar{\sigma} = \uparrow$ if $\sigma = \downarrow$ and vice versa. A time integration gives $\langle s_z(t) \rangle = \frac{\hbar}{2} \frac{1}{n_F} \sum_{\mathbf{k}} (n_{\mathbf{k}}^{\uparrow}(t) - n_{\mathbf{k}}^{\downarrow}(t))$. Contrary to Eq. (2), Eq. (4) is linear in the impurity concentration.

As we find, the form of $\langle s_z(t) \rangle$ is rather complicated, not having an exponential envelope. Still, we *define* the dephasing time T_{DP} and relaxation time T_{EY} as the time at which $\langle s(t) \rangle = \exp(-1)\langle s(0) \rangle$. Especially the EY mechanism causes an initial exponential decay with decay parameter $1/T_{\text{EY}} = 2 \sum_{\mathbf{k}\mathbf{k}'} P_{\mathbf{k}\mathbf{k}'}^{\uparrow\downarrow} / n_F$. In reality, both mechanisms act simultaneously, which should be taken into account in a full theory [27]. Here, however, we are after a separation of causes, comparing the two mechanisms as if they were independent.

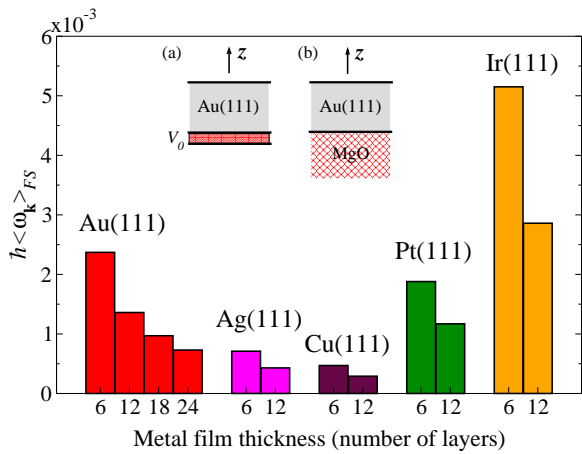


FIG. 2: (Color online) The Fermi surface average of spin-orbit field susceptibility $\hbar \langle |\boldsymbol{\omega}| \rangle$ in various metallic films as a function of film thickness. The inset shows the Au(111) film a) on the model substrate V_0 and b) on the MgO substrate.

We proceed with a presentation of our results. In Fig. 1 we show the Fermi surface distribution of the spin-orbit field susceptibility for Au(111) and Pt(111) 6-layer and 12-layer films (omitting surface states). The arrows denote the direction of the $\boldsymbol{\omega}_{\mathbf{k}}$ projected onto the surface plane while the color code shows the value of $\hbar |\boldsymbol{\omega}_{\mathbf{k}}| \times 10^3$. We find sizeable out-of-plane components of $\boldsymbol{\omega}_{\mathbf{k}}$ [26]. These must identically vanish only in the presence of in-plane inversion symmetry, $V(x, y, z) = V(-x, -y, z)$ [28], e.g. in bcc/fcc(100) or (110) systems.

The magnitude of the spin-orbit field susceptibility shows a spread, as seen from the color code. Averaging over the Fermi surface, we expect $\langle |\boldsymbol{\omega}| \rangle \propto 1/d$. Qualitatively, this behavior is indeed observed in Fig. 2 for all tested systems: Au(111), Ag(111), Cu(111), Pt(111) and Ir(111) [29]. Comparing Au(111), Ag(111) and Cu(111) at the same thickness, we find that stronger spin-orbit coupling leads to larger averaged SOF, as expected from a spin-orbit phenomenon.

For an estimation of the parameter V_0 [Eq. (3)] we calculated self-consistently a 6 ML Au(111) film on 6 layers of the wide-band-gap insulator MgO and found explicitly the SOF at high symmetry points in the Brillouin zone. A fit to $V_0 \boldsymbol{\omega}_{\mathbf{k}}$, with $\boldsymbol{\omega}_{\mathbf{k}}$ calculated for a free-standing 6-atomic-layer Au(111) film, gives us $V_0 = -12.24$ eV, which we accept as characteristic of the Au/MgO interface at all film thicknesses. Thus the Fermi surface average yields spin-orbit field of $\hbar \langle |\boldsymbol{\Omega}| \rangle = 29$ meV (for 6 layers of Pt(111) we obtain $\hbar \langle |\boldsymbol{\Omega}| \rangle = 25$ meV). The value decreases to 9 meV in a 24-atomic-layer Au(111) film, which is still considerably larger than a typical value of 1 meV met in semiconductors [8], with the consequence of a much faster spin precession in these metallic films (a splitting of $\hbar |\boldsymbol{\Omega}| = 1$ meV corresponds to a Larmor precession time of $T_L = 4.13$ ps). Different insulating substrates are expected to have different values of V_0 but in the same order of magnitude.

Now we are ready to discuss the solution of the kinetic equation (2). Fig. 3 shows the value of $\langle s_z(t) \rangle / \langle s_z(0) \rangle$ for

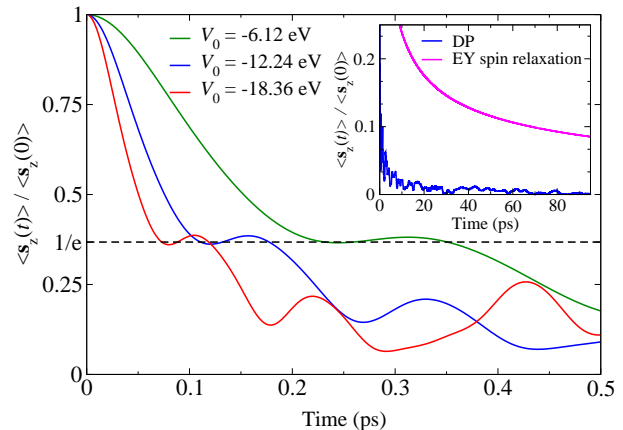


FIG. 3: (Color online) The Dyakonov-Perel time-decay of the total electron spin in 24-layer Au(111) films with 1% adatom impurities. Three cases are considered: $V_0 = -6.12$ eV, -12.24 eV and -18.36 eV. Inset: the case of $V_0 = -12.24$ eV on a larger time scale, together with the Elliott-Yafet decay.

a 24-atomic-layer Au(111) film. The adatom concentration is set to 1%. The initial rapid drop gives $T_{DP} \sim 0.1$ – 0.3 ps. The behavior is clearly oscillatory with a non-exponential envelope and with part of the signal ($\sim 2\%$ of the initial value) persisting to times as large as 80 ps, as can be seen from the inset of Fig. 3. We also explored a variation of the parameter V_0 to -6.12 eV and -18.36 eV; the qualitative behavior is the same, but with a slower or faster decay, respectively, due to the different precession frequency (see Fig. 3).

The origin of this behavior lies in the standing-wave nodal structure that the metal wavefunctions (“quantum-well states”) exhibit in the z direction (perpendicular to the film). Depending on the band, $|\Psi_{\mathbf{k}}(\mathbf{r})|^2$ can have either a negligible or a significant value in the vacuum and in the substrate. In the former case, the $\boldsymbol{\Omega}_{\mathbf{k}} \sim (\Psi_{\mathbf{k}}, V_A \Psi_{\mathbf{k}})$ almost vanishes. At these \mathbf{k} -points, the precession term in Eq. (2) is negligible even over long times. The only path to dephasing for these spins is to be scattered away first to some \mathbf{k}' with larger SOF. But since the initial state $\Psi_{\mathbf{k}}$ does not penetrate in the vacuum, the overlap with the adatom potential is also small, keeping the scattering rate low. These particular parts of the FS act in a sense as *spin traps*. Since the nodal structure of the quantum-well states depends primarily on the metallic film and not on the substrate or on the adatom, the spin traps are a property of the pristine film. However, in the presence of buried impurities instead of adatoms, or of phonons at elevated temperatures, the scattering rate will not be negligible and the spins will be scattered away from the traps at a higher rate. Additionally, the precession can freeze if $\boldsymbol{\Omega}_{\mathbf{k}}$ and $\mathbf{s}_{\mathbf{k}}$ are collinear. Since this condition is met in part of the FS (not shown) of Au(111) or Pt(111), it is part of the reason of the slow decay of s_z in these systems. We should note that the existence and effectiveness of spin traps is material and thickness dependent. Fig. 3 (inset) also shows $\langle s_z(t) \rangle / \langle s_z(0) \rangle$ by the EY mechanism (Eq. 4). Evidently, the EY spin relaxation is also affected by the spin traps, produc-

V_0 (eV)	T_{DP} (ps)			T_{EY} (ps)		T_{p} (ps)	
	-6.12	-12.24	-18.36	ws	wos	ws	wos
6-layer, 1% imp.	0.054	0.027	0.018	5.84	16.06	0.10	0.51
6-layer, 5% imp.	0.059	0.029	0.018	1.16	3.20	0.02	0.10
24-layer, 1% imp.	0.22	0.11	0.072	1.27	47.65	0.56	1.06
24-layer, 5% imp.	0.31	0.17	0.083	0.25	9.53	0.11	0.21

TABLE I: Spin-dephasing time induced by the Dyakonov-Perel mechanism, T_{DP} , in comparison to the spin-relaxation time T_{EY} induced by the Elliott-Yafet mechanism and the momentum-relaxation time T_{p} in 6-layer Au(111) and 24-layer Au(111) films with Au adatoms as scatterers. The adatom concentration is taken with respect to full surface coverage. T_{EY} and T_{p} are given with (ws) and without (wos) the surface states taken into account.

ing persisting tails, and is not exponential at large times. It is clear, however, that the DP mechanism dominates the decay process.

Table I summarizes the values of T_{DP} for 6-atomic-layer and 24-atomic-layer Au(111) with 1% and 5% of self-adatoms and for different substrate-potential values V_0 . The same Table also shows the calculated EY relaxation time, including values with (“ws”) and without (“wos”) the surface states taken into account. (The latter serves for comparing the DP and EY mechanisms acting on the same set of states.) As is qualitatively expected [8], T_{DP} increases and T_{EY} is reduced with increasing defect concentration. It is striking that T_{DP} is in all cases much lower than T_{EY} . The reason for this is basically the very high value of the spin-orbit fields causing a Larmor precession period T_{L} that is smaller than the momentum relaxation time T_{p} . E.g., for 24 layers of Au(111), $\langle |\Omega| \rangle = 9$ meV giving $T_{\text{L}} = 0.46$ ps, to be compared to $T_{\text{p}} \sim 1$ ps at 1% adatom concentration. In this regime, according to Zutić et al. [8], T_{DP} is estimated as inverse of the SOF spread $\Delta\Omega$. For 24 layers of Au(111), $T_{\text{DP}} \sim 1/\Delta\Omega = 67$ fs, which is in the same order as our first-principles value of $T_{\text{DP}} = 110$ fs. Only at much larger thicknesses does the average precession period exceed a few ps, allowing the EY mechanism to dominate [30]. Assuming that $\langle |\Omega| \rangle \propto 1/d$, we can estimate that the two mechanisms will have a comparable contribution at thicknesses of approximate 270 layers (70 nm). The DP effect, however, could be washed out at elevated temperatures, if the electron phase relaxation length becomes smaller than the film thickness so that electrons in the film interior cannot probe the substrate-surface asymmetry (different to semiconductors, the asymmetry potential does not penetrate deep into the metallic film interior due to metallic screening). In cases of weak spin-orbit coupling, e.g. Li, Na, Mg or Al, both the SOF and the spin-mixing of states are reduced proportionally to the spin-orbit strength. As a result the DP mechanism is still expected to dominate at small thicknesses, however, it is expected to enter the motional narrowing regime because of the slower Larmor precession [8].

Finally, one expects an anisotropy of the DP dephasing time with respect to the initial condition, e.g., T_{DP} will be different for $\mathbf{s}_{\mathbf{k}}(t = 0)$ perpendicular to the film compared to its

being in the film plane. This type of anisotropy has been reported previously e.g. in semiconductor heterostructures or in graphene [31] and originates from a different microscopic mechanism compared to the one reported for inversion-symmetric metals [32–34]. Using the symbol \hat{s} to denote the direction of the initial spin polarization, we have a dependence $T_{\text{DP}}(\hat{s})$ and we may define the anisotropy as the relative difference

$$\mathcal{A}_{\text{DP}} = \frac{\max_{\hat{s}} T_{\text{DP}}(\hat{s}) - \min_{\hat{s}} T_{\text{DP}}(\hat{s})}{\min_{\hat{s}} T_{\text{DP}}(\hat{s})}. \quad (5)$$

For the films studied here, \mathcal{A}_{DP} reaches values as large as 200% in a 24-atomic-layer Au(111) film. The spin traps are persistent irrespective of the initial condition, as they originate in regions of very small SOF, irrespective of the \hat{s} .

In conclusion, we find that the potential asymmetry introduced in supported metallic films by the substrate will create strong spin-orbit fields, activating the DP mechanism of spin dephasing. This effect is present in spite of the strong charge-screening in metals, since the surface and substrate are probed by the itinerant metal wavefunctions even if the potential perturbation vanishes in the film interior. We predict that the DP mechanism can dominate over the EY mechanism for thicknesses as large as 200-300 atomic layers, after which the interface induced SOF become very small, falling off inversely proportional with thickness of the film. In case of scattering only by adatoms, certain parts of the Fermi surface with low SOF acquire also low scattering rates, acting as spin traps and allowing the spin signal to persist over long times. We propose that an experiment to verify our predictions can be based on laser-pulse, pump-probe experiments (probing the Faraday or Kerr rotation) with fs temporal resolution in films of varying thickness.

We would like to thank Gustav Bihlmayer, Jaroslav Fabian and Swantje Heers for fruitful discussions. This work was financially supported by Deutsche Forschungsgemeinschaft projects MO 1731/3-1 and SPP 1538 SpinCaT, and the HGF-YIG NG-513 project of the Helmholtz Gemeinschaft. We acknowledge computing time on the supercomputers JUQUEEN and JUROPA at Jülich Supercomputing Center and JARA-HPC Compute cluster of RWTH Aachen University.

* Electronic address: h.nguyen@fz-juelich.de

† Electronic address: ph.mavropoulos@fz-juelich.de

- [1] F. J. Jedema, A. T. Filip, and B. J. van Wees, *Nature* **410**, 345 (2001).
- [2] J. Sinova, D. Culcer, Q. Niu, N. A. Sinitsyn, T. Jungwirth, and A. H. MacDonald, *Phys. Rev. Lett.* **92**, 126603 (2004).
- [3] S. O. Valenzuela and M. Tinkham, *Nature* **442**, 176 (2006).
- [4] T. Kimura, Y. Otani, T. Sato, S. Takahashi, and S. Maekawa, *Phys. Rev. Lett.* **98**, 156601 (2007).
- [5] T. Saeki, Y. Hasegawa, S. Mitani, S. Takahashi, H. Imamura, S. Maekawa, J. Nitta, and K. Takanashi, *Nat. Mater.* **7**, 125 (2008).
- [6] S.-G. Cheng, Y. Xing, Q.-F. Sun, and X. C. Xie, *Phys. Rev. B* **78**, 045302 (2008).

- [7] K. Tauber, M. Gradhand, D. V. Fedorov, and I. Mertig, Phys. Rev. Lett. **109**, 026601 (2012).
- [8] I. Zutic, J. Fabian, D. Sarma, Rev. Mod. Phys. **76**, 323 (2004).
- [9] J. Fabian, and S. Das Sarma, Phys. Rev. Lett. **81**, 5624 (1998).
- [10] R. J. Elliott, Phys. Rev. **96**, 266 (1954).
- [11] Y. Yafet, in it Solid State Physics, edited by F. Seitz and D. Turnbull (Academic, NewYork, 1963), Vol. 14, p. 1.
- [12] D. Lubzens, and S. Schultz, Phys. Rev. Lett. **36**, 1104 (1976).
- [13] M. Johnson, and R. H. Silsbee, Phys. Rev. Lett. **55**, 1790 (1985).
- [14] M. Gradhand, M. Czerner, D. V. Fedorov, P. Zahn, B. Y. Yavorsky, L. Szunyogh, and I. Mertig, Phys. Rev. B **80**, 224413 (2009).
- [15] M. Gradhand, D. V. Fedorov, P. Zahn, and I. Mertig, Phys. Rev. B **81** 020403(R) (2010).
- [16] The EY mechanism concerns spin-flip scattering events due to the spin-mixed character of Bloch states in the presence of spin-orbit coupling.
- [17] M. I. D'yakonov and V. I. Perel', Fiz. Tverd. Tela **13**, 3581 (1971) [Sov. Phys. Solid State **13**, 3023 (1972).]
- [18] G. E. Pikus, and A. N. Titkov, *Optical Orientation*, edited by F. Meier and B. P. Zakharchenya (North Holland, Amsterdam, 1984), pp. 73-131.
- [19] M. D. Mower, G. Vignale and I. V. Tokatly, Phys. Rev. B **83**, 155205 (2011).
- [20] J. Fabian, A. Matos-Abiague, C. Ertler, P. Stano, and I. Zutic, Acta Physica Slovaca **57** 565 (2007).
- [21] S. LaShell, B. A. McDougall, and E. Jensen, Phys. Rev. Lett. **77**, 3419 (1996).
- [22] J. Henk, A. Ernst, and P. Bruno, Phys. Rev. B **68**, 165416 (2003).
- [23] S. Heers, P. Mavropoulos, S. Lounis, R. Zeller, and S. Blügel, Phys. Rev. B **86**, 125444 (2012).
- [24] N. H. Long, P. Mavropoulos, B. Zimmermann, S. Heers, D. S. G. Bauer, S. Blügel and Y. Mokrousov, Phys. Rev. B **87**, 224420 (2013).
- [25] N. H. Long, P. Mavropoulos, B. Zimmermann, D. S. G. Bauer, S. Blügel, and Y. Mokrousov, Phys. Rev. B **90**, 064406 (2014).
- [26] See Supplemental Material for a detailed discussion.
- [27] P. Boross, B. Dora, A. Kiss, and F. Simon, Sci. Rep. **3**, 3233 (2013).
- [28] This is because the in-plane reflection operator R_{xy} transforms $\Psi_{\mathbf{k}}$ to $\Psi_{-\mathbf{k}}$ which is also the time-reverse state; thus the z -component of the spin, s_z , must flip by time-reversal. At the same time, $R_{xy}\sigma_z R_{xy}^{-1} = +\sigma_z$, i.e., s_z must be conserved. This leads to $s_z = 0$, i.e., also $(\Omega_{\mathbf{k}})_z = 0$.
- [29] This trend can be violated at specific \mathbf{k} -points, as was shown e.g. for Pb films on Si, (see. J. H. Dil, F. Meier, J. Lobo-Checa, L. Patthey, G. Bihlmayer, and J. Osterwalder, Phys. Rev. Lett. **101**, 266802 (2008)).
- [30] T_p is, to a first approximation, independent of the film thickness: the scattering matrix element off impurities scales as $\propto 1/d$, but the number of available final states increase as $\propto d$.
- [31] S. Fratini, D. Gosálbez-Martínez, P. Merodio Cámara, and J. Fernández-Rossier, Phys. Rev. B **88**, 115426 (2013).
- [32] B. Zimmermann, P. Mavropoulos, S. Heers, N. H. Long, S. Blügel and Y. Mokrousov, Phys. Rev. Lett. **109**, 236603 (2013).
- [33] Y. Mokrousov, H. Zhang, F. Freimuth, B. Zimmermann, N. H. Long, J. Weischenberg, I. Souza, P. Mavroupos, and S. Blügel, J. Phys.: Condens. Matter **25**, 163201 (2013).
- [34] N. H. Long, P. Mavropoulos, S. Heers, B. Zimmermann, Y. Mokrousov, and S. Blügel, Phys. Rev. B **88**, 144408 (2013).